Available online at www.sciencedirect.com
SCIENCE DIRECT
Electrochimica Acta 51 (2006) 4352–4357
ELECTROCHIMICA Acta
www.elsevier.com/locate/electacta

Improvement of electrochemical properties of $LiNi_{0.5}Mn_{1.5}O_4$ spinel prepared by radiated polymer gel method

H.Y. Xu, S. Xie, N. Ding, B.L. Liu, Y. Shang, C.H. Chen *

Department of Materials Science and Engineering, University of Science and Technology of China, Anhui, Hefei 230026, PR China

Received 13 October 2005; received in revised form 12 December 2005; accepted 13 December 2005
Available online 19 January 2006

Abstract

$LiNi_{0.5}Mn_{1.5}O_4$ as a 4.7 V-class cathode material was prepared through the radiated polymer gel method that allowed homogeneous mixing of starting materials at the atomic scale. After calcinations of the polymer gels containing the metal salts at different temperatures from 750 to 1150 °C, powders of a pure $LiNi_{0.5}Mn_{1.5}O_4$ phase were obtained. X-ray diffraction and transmission electron microscopy were used to characterize the structures of the powders. Galvanostatic cell cycling and a simultaneous DC resistance measurement were performed on Li/$LiNi_{0.5}Mn_{1.5}O_4$ cells. It is found that the powder calcined at 950 °C shows the best electrochemical performance with the initial discharge capacity of 139 mAh g^{-1} and 96% retention after 50 cycles. Adopting a slow cooling procedure for the powder calcination can increase the capacity of $LiNi_{0.5}Mn_{1.5}O_4$ at the 4.7 V plateau. Besides, a "w"-shape change of the DC resistance of Li/$LiNi_{0.5}Mn_{1.5}O_4$ cells is a good indication of the structural change of $LiNi_{0.5}Mn_{1.5}O_4$ electrode during charge and discharge courses.

Keywords: Lithium nickel manganese oxide; Spinel; Lithium battery; Electrode; Radiated polymer gel

1. Introduction

Lithium secondary batteries based on $LiCoO_2$ cathode and graphite anode have proved to be the best power sources for portable electronic devices because of their high output voltages, high specific energy densities, and excellent cycling performance. However, there is a further demand for even higher specific energy density for use in large devices such as electric vehicles. One plausible solution to such an energy density issue is to use cathode materials with higher working voltages. It is well known that $LiCoO_2$, $LiNiO_2$, and $LiMn_2O_4$ are combined with carbon anode materials to make 4.0 V rechargeable lithium-ion batteries [1–7]. Among them, the spinel-type $LiMn_2O_4$ has been investigated as a cheap cathode material because Mn-containing precursors are usually much cheaper than Co-precursors [3,5,6]. However, plain $LiMn_2O_4$ is not stable during the discharge and charge cycles in batteries. Therefore, much research has been performed to improve its cycling performance. An effective strategy is the partial substitution of Mn ions with other transition metal ions such as Ti, Cr, Fe, Co, Ni, Cu and Zn [8,9], and Er [10]. During the course of these studies, it has been found that a Ni-substituted spinel manganese oxide, i.e. $LiNi_{0.5}Mn_{1.5}O_4$, has exhibited the desired discharge and charge behavior in the 5.0 V regions [8,9].

So far, many chemical routes have been used to synthesize spinel $LiNi_{0.5}Mn_{1.5}O_4$ powders and thin films. These synthesis methods include solid-state reaction [9], sol–gel [11], emulsion drying [12], electrostatic spray deposition [13], composite carbonate process [14,15], ultrasonic spray pyrolysis [16], and molten salt process [17]. It can be concluded from these earlier studies that most of these routes do not produce a pure phase $LiNi_{0.5}Mn_{1.5}O_4$ but rather often with impurities of nickel oxides. For the few methods that result in pure $LiNi_{0.5}Mn_{1.5}O_4$ phase, such as composite carbonate process [14,15] and ultrasonic spray pyrolysis [16], they are too complicated to be easily applied in actual large-scale production.

On the other hand, $LiNi_{0.5}Mn_{1.5}O_4$ is found to have two different crystal structures of the space groups of *Fd3m* in which Mn ions are present in mainly Mn^{4+} and minor Mn^{3+}, and $P4_332$ in which Mn ions are only present in Mn^{4+} [18]. It is considered that the $LiNi_{0.5}Mn_{1.5}O_4$ of *Fd3m* space group can be converted to that of $P4_332$ space group by means of a post-annealing pro-

* Corresponding author. Tel.: +86 551 3602938; fax: +86 551 3602940.
E-mail address: cchchen@ustc.edu.cn (C.H. Chen).

0013-4686/$ – see front matter © 2005 Elsevier Ltd. All rights reserved.
doi:10.1016/j.electacta.2005.12.014

cess [11,16,18]. The annealing readily changes the oxidation state of Mn from 3+ to 4+, leading to the production of perfect $LiNi_{0.5}^{2+}Mn_{1.5}^{4+}O_4$ crystal structure. Nevertheless, according to Kim et al.'s studies [18], $LiNi_{0.5}Mn_{1.5}O_4$ of *Fd3m* space group has superior electrochemical behavior and structure reversibility compared to $LiNi_{0.5}Mn_{1.5}O_4$ with $P4_332$ space group. Thus, we have been mostly targeting the $LiNi_{0.5}Mn_{1.5}O_4$ with *Fd3m* space group in our investigations.

In our previous study, we have succeeded in preparing $LiCoO_2$ powder through a novel radiated polymer gel method (RPG) [19]. It is similar to the sol–gel method, but without the sol-to-gel step. Instead, we directly obtain a polymer gel that contains precursor salts by using γ-ray irradiation to initiate the polymerization of an organic monomer solution. In this method, the formation of the gel is quick and easy to control, and, most importantly, the precursors are mixed very homogeneously in the gel that can be transformed into a cathode powder after high-temperature calcination.

In this study, we adopt this simple and excellent synthetic method RPG to synthesize $LiNi_{0.5}Mn_{1.5}O_4$. Meanwhile, we compare the effect of two different cooling procedures on the structure and electrochemical performance of the $LiNi_{0.5}Mn_{1.5}O_4$ powders. We have also found that a "w"-shape change of the DC resistance of $Li/LiNi_{0.5}Mn_{1.5}O_4$ cells is a good indication of the structural change of $LiNi_{0.5}Mn_{1.5}O_4$ electrode during charge and discharge courses.

2. Experimental

$LiNO_3$, $Ni(NO_3)_2{\cdot}6H_2O$, and $Mn(CH_3COO)_2{\cdot}4H_2O$ were dissolved in deionized water in the molar ratio of Li:Ni:Mn = 1.06:0.5:1.5 to obtain a 0.5 mol/L solution, then acrylic acid (AA) (CH_2=CHCOOH) was added to form an AA–H_2O (1:2, v/v) solution, the pH value of which was about 2. The solution was polymerized under the condition of Co60 γ-ray irradiation (intensity 55–75 Gy/min) for 5 h. Thus, a green and homogeneous poly(acrylic acid) gel was obtained. The gel was heated at 140 °C for 8 h to get rid of the impregnated water and AA residue. A subsequent heat treatment was carried out at 750–1150 °C in air for 10 h followed by a natural cooling step (approximately 80 °C/h cooling rate) to obtain $LiNi_{0.5}Mn_{1.5}O_4$ powders. To investigate the effect of cooling rate, we also adopted a slow cooling step (approximately 12 °C/h cooling rate) for the sample calcined at 950 °C.

The crystalline structure of the samples was characterized by X-ray diffraction (XRD) using a diffractometer (Philips X'Pert Pro Super, Cu Kα radiation). The diffraction patterns were recorded at room temperature in the 2θ range from 10° to 70°. The powder sintered at 950 °C was also analyzed under a transmission electron microscope (TEM, 200 kV; Hitachi H-800).

Electrode laminates for the electrochemical testing were prepared by casting a slurry consisting of a $LiNi_{0.5}Mn_{1.5}O_4$ powder (75 wt.%), acetylene black (15 wt.%), and poly(vinylidene fluoride) (PVDF) (10 wt.%) dispersed in 1-methyl-2-pyrrolidinone (NMP) onto an aluminum foil. The laminates were then dried at 70 °C for 2 h. The $Li/LiNi_{0.5}Mn_{1.5}O_4$ coin-cells (2032 size) were made with 1 M $LiPF_6$ in ethylene carbonate (EC):diethyl carbonate (DMC) (1:1, w/w) as the electrolyte. The cells were tested on a multi-channel battery cycler (Shenzhen Neware Co. Ltd.) and subjected to charge–discharge cycles at 0.2 mA cm^{-2}, respectively, between 3.0 and 5.1 V (versus Li metal).

The internal resistance of the cells was also measured by a current interruption technique. This was done by cutting off the current intermittently for 1 min through the process of charge and recording the voltage change before and after interruption. Thus, the DC resistance of a cell (R_{dc}) at a certain state-of-charge (SOC) or depth of discharge (DOD) can be calculated as $R_{dc} = \Delta U/\Delta I$.

3. Results and discussion

3.1. Structure analysis

Based on Kim et al.'s study [18], crystal structure of $LiNi_{0.5}Mn_{1.5}O_4$ with cubic spinel structure (*Fd3m*) is illustrated in Fig. 1A, where Li ions are in 8a sites, Ni and Mn ions in 16d sites, and O ions in 32e sites. Note that stoichiometric number of O ions is assumed in this drawing although there may be some oxygen deficiency in the samples calcined in air or an oxygen-poor atmosphere [12]. In addition, the Ni and Mn ions are assumed to be randomly distributed on 16 sites. Fig. 1B shows the XRD patterns of the $LiNi_{0.5}Mn_{1.5}O_4$ powders obtained by calcining the radiated gel at a temperature from 750 to 1150 °C. It can be seen that the calcinations at 750, 850, 950, and 1050 °C in air have produced a single phase of $LiNi_{0.5}Mn_{1.5}O_4$ with cubic spinel structure (*Fd3m*). Here, we show that the single phase

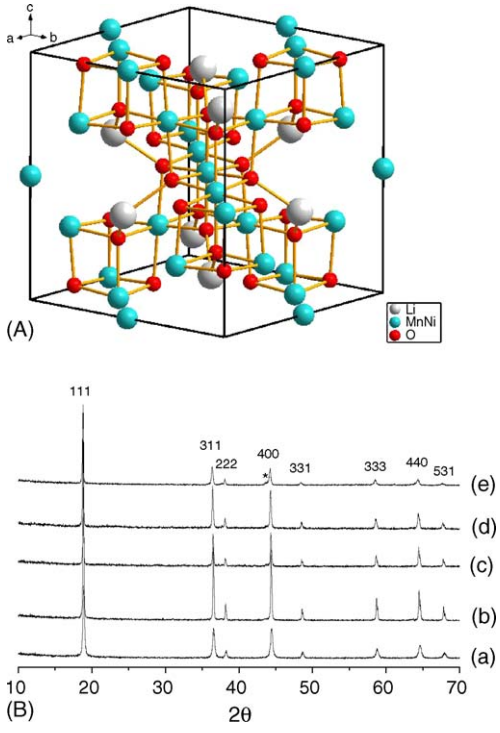

Fig. 1. Crystal structure of $LiNi_{0.5}Mn_{1.5}O_4$ having *Fd3m* space group (A), and X-ray diffraction patterns of $LiNi_{0.5}Mn_{1.5}O_4$ calcined at 750 °C (a), 850 °C (b), 950 °C (c), 1050 °C (d), and 1150 °C (e). The peak indicated by a star is from the diffraction of NiO or Li_xNi_yO (B).

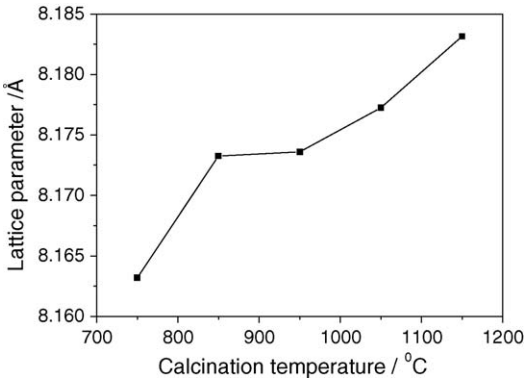

Fig. 2. The lattice parameter of $LiNi_{0.5}Mn_{1.5}O_4$ powders as a function of the calcination temperature.

of $LiNi_{0.5}Mn_{1.5}O_4$ can be easily prepared by the RPG method without any repeated calcination steps. This is due to the advantage of very homogeneous mixing of the cations, i.e. Li, Ni, and Mn ions, in the gel precursor. However, when the calcination temperature is as high as 1150 °C (pattern e), a small amount of impurity phase that may be assigned to NiO or Li_xNi_yO is also detected in the sample. The appearance of the impurity phase is likely related to the loss of lithium at high temperatures. This phenomenon is different from that found in a solid-state reaction [9], where impurity phases appear at a relatively low sintering temperature.

In addition, based on these XRD patterns the lattice parameters can be calculated by Unit Cell software based on the least-square method. The result is shown in Fig. 2. It is obvious that with increasing the calcination temperature from 750 to 1150 °C, the lattice parameter increases monotonously. As mentioned above, oxygen deficiency in the product occurs at high temperatures [12]. Thus, as long as oxygen loss takes place, the average manganese valence would decrease owing to the charge balance compensation, implying some small portion of Mn^{4+} is reduced to Mn^{3+}, resulting in the lattice parameter increasing with increasing calcination temperature.

The TEM image of the powder calcined at 950 °C is shown in Fig. 3. The particles are irregular-shaped and the particle size is in the range of 80–200 nm. The particle morphology of the powders calcined at other temperatures is similar to the 950 °C-calcined powder. The irregular shape is expected because the particles are formed by the breaking-down and burning-out of polymer gels.

3.2. Electrochemical performance

The charge–discharge profiles of $Li/LiNi_{0.5}Mn_{1.5}O_4$ cells cycled between 3.0 and 5.1 V at 30 °C are presented in Fig. 4. It can be seen that except for the $LiNi_{0.5}Mn_{1.5}O_4$ powder calcined at 750 °C that only shows the 4.7 V plateau, all of the other cells made with $Li/LiNi_{0.5}Mn_{1.5}O_4$ electrodes reveal a long 4.7 V plateau and a short 4 V plateau. The 4.7 V plateau is caused by the redox reactions of Ni^{2+}/Ni^{4+}, while the 4.0 V plateau is caused by the redox reactions of Mn^{3+}/Mn^{4+} [8]. The 950 °C-calcined $LiNi_{0.5}Mn_{1.5}O_4$ powder delivers both the highest overall capacity and the 4.7 V-plateau capacity among all the cells using $LiNi_{0.5}Mn_{1.5}O_4$ calcined at five different temperatures as the cathode materials. Furthermore, its discrepancy between the charge and discharge voltage plateaus is the smallest, which probably means a minimum cell impedance for it. Therefore, even though a single $LiNi_{0.5}Mn_{1.5}O_4$ phase is formed, there may exist Mn^{3+} ions in the product. Apparently, there is no Mn^{3+} existing in the 750 °C-calcined powder owing to no oxygen loss at the low calcination temperature. This is consistent with Myung et al.'s study where they have found that a low sintering temperature is in favor of reducing the amount of Mn^{3+} in the spinel structure [12].

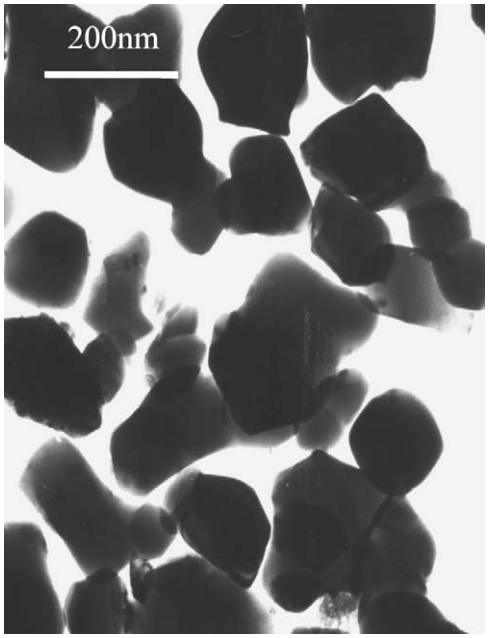

Fig. 3. TEM image of the $LiNi_{0.5}Mn_{1.5}O_4$ powder calcined at 950 °C for 10 h.

Fig. 5 shows the overall discharge capacity (Fig. 5a) and 4.7 V-plateau capacity, which is defined in this study by the discharge capacity above 4.2 V (Fig. 5b), with the cycle number for the $Li/LiNi_{0.5}Mn_{1.5}O_4$ cells. It can be seen that the 950 °C-calcined $LiNi_{0.5}Mn_{1.5}O_4$ delivers a capacity of 139 mAh g^{-1}

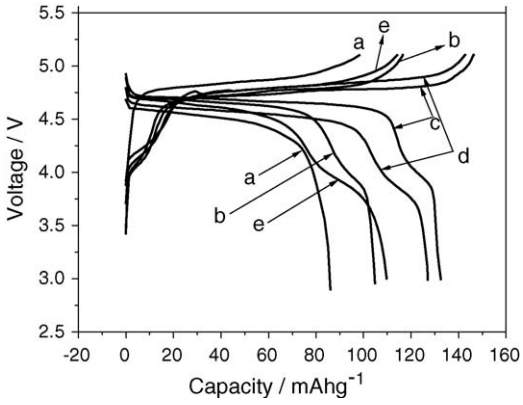

Fig. 4. Charge–discharge curves for $Li/LiNi_{0.5}Mn_{1.5}O_4$ cells with $LiNi_{0.5}Mn_{1.5}O_4$ calcined at 750 °C (a), 850 °C (b), 950 °C (c), 1050 °C (d), and 1150 °C (e). The current density was 0.2 mA cm^{-2}.

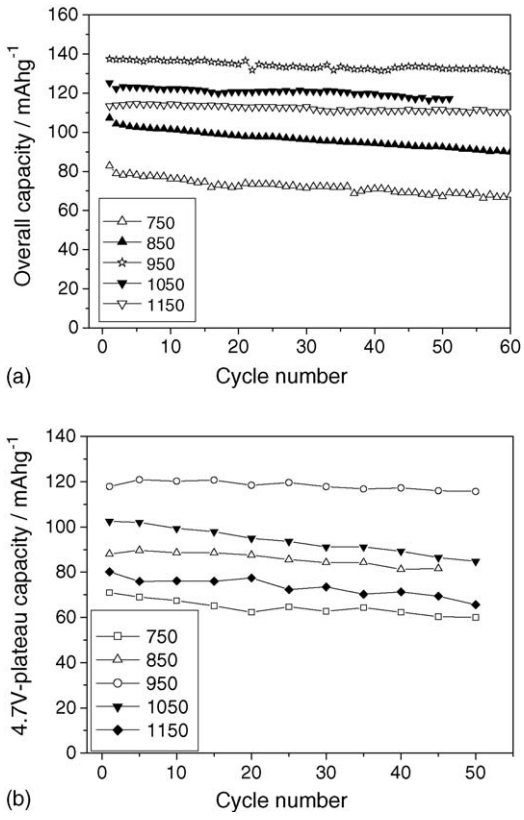

Fig. 5. The overall discharge capacity (a) and 4.7 V-plateau capacity (b) of $Li/LiNi_{0.5}Mn_{1.5}O_4$ cells at the current density of 0.2 mA cm^{-2}. The 4.7 V-plateau capacity is defined as the capacity above 4.2 V.

in the first cycle and retains 96% of the initial capacity after 50 cycles (Fig. 5a). This result is very close to the theoretical capacity of $LiNi_{0.5}Mn_{1.5}O_4$, i.e. 146 mAh g^{-1}, and is among the best data ever reported in literature [12,15]. It is also noticed that with increasing the calcination temperature from 750 to 950 °C, the capacity first increases and reaches a maximum at the calcination temperature of 950 °C; then it decreases with increasing the calcination temperature from 1050 to 1150 °C. The 4.7 V-plateau capacity follows the same trend (Fig. 5b). Obviously, the powder calcined at 950 °C still gives rise to the highest 4.7 V-plateau capacity with 120 mAh g^{-1} in the first cycle. It is around 70, 90, 100, and 80 mAh g^{-1}, respectively, for the $LiNi_{0.5}Mn_{1.5}O_4$ samples calcined at 750, 850, 1050, and 1150 °C. This trend can be understood by considering the change of crystallinity and the stoichiometry of the calcined powders. The higher calcination temperature leads to higher crystallinity (Fig. 1B) that helps to increase the electrode capacity. On the other hand, too high calcination temperature may be accompanied by oxygen loss and the appearance of impurity phases such as NiO. Therefore, with the combination of these two factors, 950 °C happens to be the optimal calcination temperature.

A typical discharge voltage profile with a simultaneous current interruption measurement is given by Fig. 6a. The spikes on the curve are due to the rapid voltage rises when the current is cut into zero. The shape of the voltage response is also inserted in Fig. 6a. DC resistance of the cells versus the state-of-charge, which is defined as the ratio (in percentage) of the actual charged capacity during a charge step to the overall achievable charge capacity, is shown in Fig. 6b. Obviously, among all the cells, the one using the 950 °C-calcined $LiNi_{0.5}Mn_{1.5}O_4$ demonstrates minimum resistance. This is also a reason why this cell can achieve the maximum capacity (Fig. 5). In addition, except for the cell using 750 °C-calcined $LiNi_{0.5}Mn_{1.5}O_4$, other cells show the same pattern of the resistance versus SOC relationship. In the beginning stage of the charge step, cell resistance increases quite rapidly and reaches a maximum at the SOC of 10–20%. Then the resistance quickly drops to a relatively low value and then it undergoes small changes for the rest of the charge step. A careful observation on the curve shape leads us to conclude that the curves for the rest of charge step can be roughly evenly divided into two segments, which is probably corresponding to the Ni^{2+}/Ni^{3+} transition before 50% SOC and the Ni^{3+}/Ni^{4+} transition after 50% SOC. Such a division is more obvious if we plot the DC resistance against the cell voltage at which the current interruption starts (Fig. 6c). We can clearly see that each curve has two minimum resistance values at around 4.7 V, forming a "w"-shape curve part. Theoretically, this resistance versus voltage (*R–V*) curve is very similar to the cyclic voltammogram of a cell, but it can be obtained during a simultaneous measurement of the galvanostatic capacity of a cell. Considering the fact that the voltage profiles of the cells do not show clearly the two-plateau characteristics at around 4.7 V (Fig. 4), the appearance of the "w"-shape *R–V* curve indicates that this simultaneous DC resistance measurement is very sensitive to the structural change of the electrode. Alternatively, the 4.7 V two-plateau feature of $Li/LiNi_{0.5}Mn_{1.5}O_4$ cells has been also probed with cyclic voltammetry [13,18,20]. As for the far higher resistance for the cell using 750 °C-calcined $LiNi_{0.5}Mn_{1.5}O_4$ as cathode than other cells, it is mostly resulted from its relatively poor crystallinity of the cathode powder (Fig. 1B).

In order to prolong the 4.7 V plateau and suppress the 4.0 V plateau, we adopted a slow cooling procedure for the 950 °C-calcined $LiNi_{0.5}Mn_{1.5}O_4$ powder to increase its oxygen content. Cyclic voltammograms (CV) of $Li/LiNi_{0.5}Mn_{1.5}O_4$ cells using fast-cooled (or called natural-cooled in this study) and slowly cooled $LiNi_{0.5}Mn_{1.5}O_4$ samples in the second cycle are given in Fig. 7a. It is clear that the relative peak intensity ratio between the 4 V peak and 4.7 V peak of the $Li/LiNi_{0.5}Mn_{1.5}O_4$ (slowly cooled) cell is much smaller than that of the $Li/LiNi_{0.5}Mn_{1.5}O_4$ (fast-cooled) cell. Fig. 7b shows cycling characteristics of $Li/LiNi_{0.5}Mn_{1.5}O_4$ cells made with two kinds of 950 °C-calcined $LiNi_{0.5}Mn_{1.5}O_4$ powders obtained by natural cooling and slow cooling procedures, respectively. It can be seen from the charge–discharge profiles (Fig. 7b) that the 4.0 V plateau becomes very shorter for the slowly cooled $LiNi_{0.5}Mn_{1.5}O_4$. The relationships of capacity versus cycle number of the cells are also shown in Fig. 7c. It is noticed that the slowly cooled $LiNi_{0.5}Mn_{1.5}O_4$ shows a little lower overall capacity than that of fast-cooled sample. However, its capacity at 4.7 V plateau is between 120 and 126 mAh g^{-1} during 50 cycles, which is about 10 mAh g^{-1} higher than that of fast-cooled sample. Hence, the synthesis of $LiNi_{0.5}Mn_{1.5}O_4$ via a slow cooling step is a simple and effective method to improve the capacity at 4.7 V.

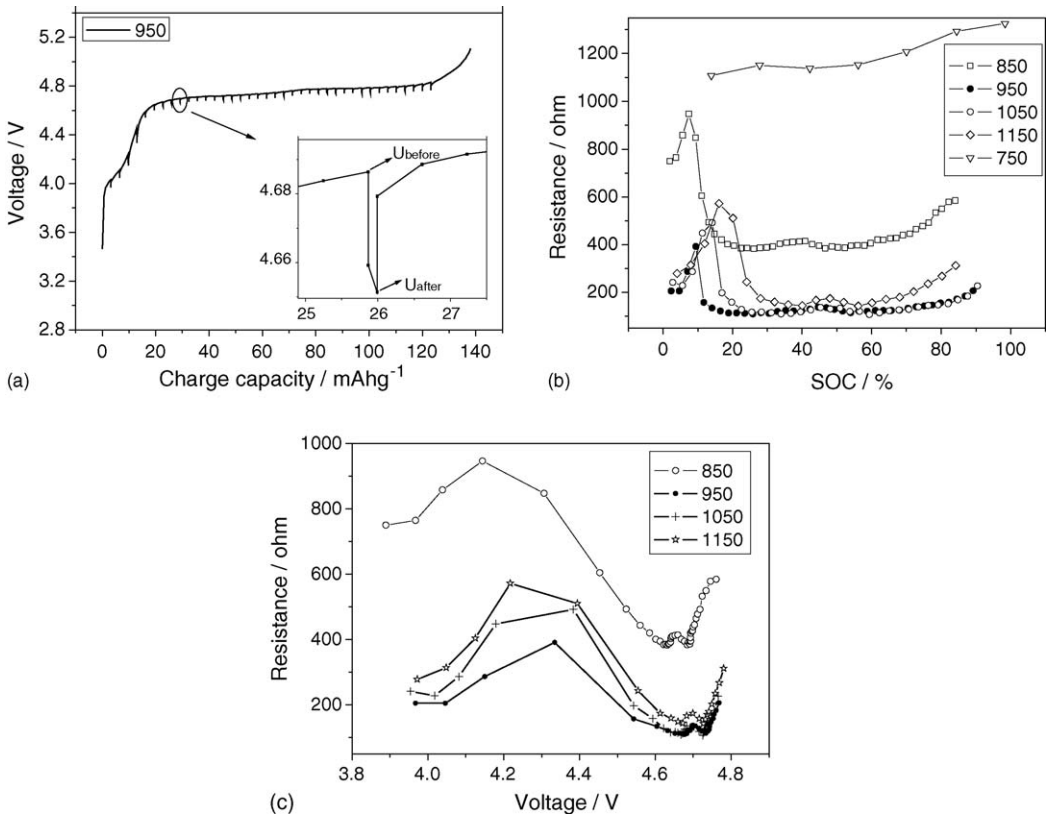

Fig. 6. A charge profile of a Li/$LiNi_{0.5}Mn_{1.5}O_4$ cell using 950 °C-calcined $LiNi_{0.5}Mn_{1.5}O_4$ samples with a simultaneous current interruption measurement (a), the direct current resistance as a function of state of charge (b) and as a function of cell voltage (c).

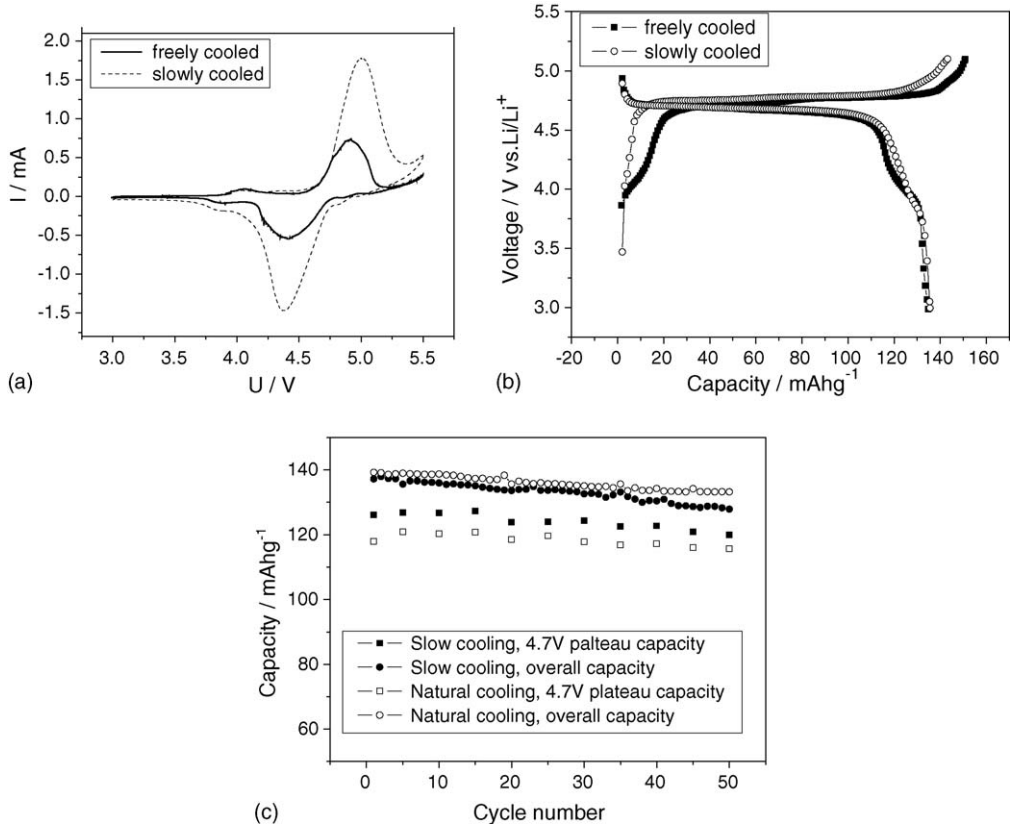

Fig. 7. Electrochemical characteristics of Li/$LiNi_{0.5}Mn_{1.5}O_4$ cells with $LiNi_{0.5}Mn_{1.5}O_4$ prepared by natural cooling (80 °C/h) and slow cooling (12 °C/h), respectively: cyclic voltammograms (a), voltage profile (b), and capacity vs. cycle number relationship (c).

4. Conclusions

In this paper, the 4.7 V-cathode $LiNi_{0.5}Mn_{1.5}O_4$ powders have been prepared with radiated polymer gel method. The electrochemical properties of these powders are closely related to the calcination temperature. The sample calcined at 950 °C shows the best electrochemical performance with an initial capacity of 139 mAh g^{-1} and 96% capacity retention after 50 cycles. Adopting a slow cooling procedure during the powder calcinations can increase the capacity of $LiNi_{0.5}Mn_{1.5}O_4$ at the 4.7 V plateau. In addition, a "w"-shape change of the DC resistance of Li/$LiNi_{0.5}Mn_{1.5}O_4$ cells is a good indication of the structural change of $LiNi_{0.5}Mn_{1.5}O_4$ electrode during charge and discharge courses.

Acknowledgements

This study was supported by 100 Talents Program of Academia Sinica and National Science Foundation of China (Grant Nos. 50372064 and 20471057). We are also grateful to the China Education Ministry (SRFDP No. 20030358057). The USTC Radiation Chemistry Laboratory has provided the assistance for the polymer gel synthesis.

References

[1] D. Guyomard, J.M. Tarascon, J. Electrochem. Soc. 139 (1992) 937.
[2] T. Ohzuku, A. Ueda, M. Nagayama, J. Electrochem. Soc. 140 (1993) 1862.
[3] C.D.W. Jones, E. Rossen, J.R. Dhan, Solid State Ionics 68 (1994) 65.
[4] K. Ozawa, Solid State Ionics 69 (1994) 212.
[5] A. Yamada, K. Miura, K. Hinokuma, M. Tanaka, J. Electrochem. Soc. 142 (1995) 2149.
[6] Y. Gao, J.R. Dhan, J. Electrochem. Soc. 143 (1996) 100.
[7] T. Ohzuku, A. Ueda, J. Electrochem. Soc. 144 (1997) 212.
[8] T. Ohzuku, S. Takeda, M. Iwanaga, J. Power Sources 81 (1999) 90.
[9] K. Kanamura, W. Hoshikawa, T. Umegaki, J. Electrochem. Soc. 149 (2002) A339.
[10] H.W. Liu, L. Song, K.L. Zhang, Inorg. Mater. 41 (2005) 646.
[11] X.L. Wu, S.B. Kim, J. Power Sources 109 (2002) 53.
[12] S.T. Myung, S. Komaba, N. Kumagai, H. Yashiro, H.T. Chung, T.H. Cho, Electrochim. Acta 47 (2002) 2543.
[13] M. Mohamedi, M. Makino, K. Dokko, T. Dokko, T. Itoh, I. Uchida, Electrochim. Acta 48 (2002) 79.
[14] Y.S. Lee, Y.K. Sun, S. Ota, T. Miyashita, M. Yoshio, Electrochem. Commun. 4 (2002) 989.
[15] G.Q. Liu, Y.J. Wang, L. Qi, W. Li, H. Chen, Electrochim. Acta 50 (2005) 1965.
[16] S.H. Park, Y.K. Sun, Electrochim. Acta 50 (2004) 431.
[17] J.H. Kim, S.T. Myung, Y.K. Sun, Electrochim. Acta 49 (2004) 220.
[18] J.H. Kim, S.T. Myung, C.S. Yoon, S.G. Kang, Y.K. Sun, Chem. Mater. 16 (2004) 906.
[19] N. Ding, X.W. Ge, C.H. Chen, Mater. Res. Bull. 40 (2005) 1451.
[20] B. Markovsky, Y. Talyossef, G. Salitra, D. Aurbach, H.J. Kim, S. Choi, Electrochem. Commun. 47 (2002) 2543.